Available online at www.sciencedirect.com

ScienceDirect

Geochimica et Cosmochimica Acta 283 (2020) 124–135

Geochimica et Cosmochimica Acta

www.elsevier.com/locate/gca

A quantitative and mechanistic model for the coupling between chemistry and clay hydration

Nicolas C.M. Marty [a,*], Sylvain Grangeon [a], Arnault Lassin [a], Benoit Madé [b], Philippe Blanc [a], Bruno Lanson [c]

[a] BRGM, 3 Avenue Guillemin, Orléans Cedex 2 45060, France
[b] Andra, 1/7 Rue Jean Monnet, 92298 Châtenay-Malabry, France
[c] Univ. Grenoble Alpes, CNRS, Univ. Savoie Mont Blanc, IRD, Univ. Gustave Eiffel, ISTerre, F-38000 Grenoble, France

Received 10 February 2020; accepted in revised form 27 May 2020; Available online 3 June 2020

Abstract

It is proposed here to describe smectite water vapor desorption isotherms using an exchange formalism that quantitatively accounts for the different hydration states and thus different water contents. This approach makes it possible to reproduce both desorption isotherms and relative proportions of the different hydration states as determined by X-ray diffraction. The method is numerically robust and easy to implement in most reactive transport codes. The formalism is satisfactory from a phenomenological point of view and accounts for the influence of external parameters such as interlayer cation composition and solution cation composition and salinity on clay hydration. Furthermore, in contrast to most solid solution models, this approach focuses on the clay reactivity according to the charge and type of interlayer cation rather than on its solubility and therefore does not require the overall thermodynamic properties of the clay. In addition, such an explicit distinction of the hydration/cation exchange processes from the thermodynamic stability of smectite 2:1 layer allows the use of kinetics driving slow dissolution/precipitation rates if the number of exchange sites is related to the amount of clay minerals.

Keywords: Clay composition; Ionic strength; Hydration model; Exchange reaction; Gapon; Rothmund-Kornfeld

1. INTRODUCTION

The crystal structure of clay minerals can be described as the parallel stacking of layers separated from each other by an interlayer space. Smectite, a generic name that encompasses several minerals (Guggenheim et al., 2006), is one of the most abundant type of clay minerals in various natural settings, including soils and sediments (Griffin et al., 1968; Jackson, 1957; Murray and Leininger, 1955), together with illite and chlorite. The general layer structure of smectite can be described as two tetrahedral sheets sandwiching an octahedral sheet. In the octahedral sheet, cations can be mainly divalent (trioctahedral smectite) or trivalent (dioctahedral smectite). The isomorphic substitution of a cation by another of lower valence (e.g. Al^{3+} for Si^{4+} in the tetrahedral sheet, Mg^{2+} for Al^{3+} or Li^{+} for Mg^{2+} in the octahedral sheet) gives rise to a permanent layer charge that is compensated for by the presence of hydrated cations in the interlayer space. Vermiculite has a similar layer structure and differs from smectite by its higher layer charge deficit [1.2–1.8 and 0.4–1.2 charge equivalent per $O_{20}(OH)_4$ in vermiculite and smectite, respectively – Guggenheim et al. (2006)]. This charge contrast does not appear to induce significant modification of the hydration behavior or of the distribution of interlayer species (Dazas et al., 2015; Vinci et al., 2020). Both families of swelling phyllosilicates are thus hereafter jointly referred to as "smectite". The classification of

* Corresponding author.
E-mail address: n.marty@brgm.fr (N.C.M. Marty).

https://doi.org/10.1016/j.gca.2020.05.029
0016-7037/

smectite minerals is based on multiple criteria and takes into account the tri- or dioctahedral character of the octahedral sheets, the location of the layer charge (tetrahedral or octahedral), and the density of the layer charge (Guggenheim et al., 2006). For example, saponite is a trioctahedral smectite with tetrahedral layer charge, hectorite is a trioctahedral smectite with octahedral layer charge, and montmorillonite is a dioctahedral smectite with octahedral layer charge. The density and location of the layer charge influences not only smectite cation uptake capacity and the relative affinity of different cations for its surface, but also smectite hydration properties (Sato et al., 1992; Vinci et al., 2020). In turn, hydration and dehydration properties influence smectite swelling and shrinkage properties (e.g. Norrish, 1954). Indeed, smectite hydration involves the uptake of interlayer water, i.e. the intercalation of a variable number of water molecules in the initially anhydrous interlayer (hereafter referred to as the "0W" state). These water molecules are organized to form 1, 2, or 3 "planes" parallel to the layer plane (hereafter denominated "1W", "2W", and "3W", respectively), with the most hydrated interlayer having the highest number of "water planes" and the highest layer-to-layer distance. These interlayer hydration states often coexist within a given crystal, and the structure is then described as "interstratified", with distinct interlayer spaces hosting different number of water planes. The quantitative understanding of clay hydration thus requires not only the modelling of the total amount of water sorbed as a function of the relative humidity, but also the quantification of the relative abundances of the different hydration states. This ability to model clay hydration is a fundamental stage in the development of THMC (Thermal–Hydraulic–Mechanical–Chemical) codes, which aim to couple chemistry, thermal, hydraulic and mechanical effects to be as realistic as possible, and thus require the link between layer charge and hydration to be quantitatively assessed.

To describe the water desorption/adsorption isotherms on clays, numerous studies used the solid solution model based on Ransom and Helgeson (1994) (e.g. Dubacq et al., 2009; Vidal and Dubacq, 2009; Tajeddine et al., 2015; Vieillard et al., 2011, 2019; Gailhanou et al., 2017). Although solid solutions, or the consideration of discretized clay end-members with different hydration states, can be employed to describe the water content of clays, the practical implementation of this approach in reactive transport codes remains difficult. These models require indeed the thermodynamic properties of each end-member to be known, i.e. each hydration state, for each layer charge and each interlayer cation, has to be characterized together with possible interaction parameters between end-members (e.g. Margules parameters). Furthermore, most of these models focus on clay formation or stability, and therefore include thermodynamic properties of clay layers (i.e. standard Gibbs energy of formation). As changes in hydration state are relatively rapid processes (e.g. Bray et al., 1998), solid solutions that relate the stability of clay layers are thus incompatible with the use of kinetics driving slow dissolution/precipitation rates of clay minerals (e.g. Marty et al., 2018). Another drawback of the solid solution approach when applied to geochemical modelling is the requirement for the cross-linked thermodynamic equilibrium of both the clay layer and the interlayer cation composition with the contacting solution. As an alternative to these thermodynamic models, Freundlich's model and the BET model (Brunauer, Emmett and Teller) (e.g. Hatch et al., 2012; Revil and Lu, 2013), as well as other equations described in Arthur et al. (2016), are commonly used to reproduce clay desorption/adsorption isotherms. Despite significant efforts (e.g. Lindholm et al., 2019), the lack of mechanistic constraints relating the chemical properties of clay makes the Mechanical–Chemical coupling uncertain, however. Most limitations of the above-described modelling approaches can be circumvented by molecular modelling techniques, which are increasingly used to study the conformation of atoms in the structure (e.g. Ferrage et al., 2011; Dazas et al., 2015), including the dynamics of interlayer cations and water (e.g. Holmboe and Bourg, 2014; Rotenberg et al., 2007). Despite its numerous advantages (sound mechanistic foundations, capacity to probe the kinetics of ion exchange, capacity to predict), the large computational expense required makes molecular modelling incompatible with large scale reactive transport simulations.

The present study aims to develop an alternative model focused on clay reactivity (i.e. hydration and cation exchange) which is both numerically robust and easy to implement in geochemical codes, for example to reproduce diagenetic processes (e.g. Tremosa et al., 2020), soil shrink-swell (e.g. Cornelis et al., 2006), soil water availability (e.g. Rawls et al., 1991) or the fate of clays at a radioactive waste disposal site (e.g. Marty et al., 2014). The proposed model is based on the Gapon convention (Gapon, 1933) and uses the exchange reaction formalism (i.e. approach similar to an ideal solid solution) to quantitatively reproduce water desorption isotherms, including total water content and clay hydration heterogeneity (i.e. proportions of 0 W, 1 W, 2 W, and 3 W hydrates within a given crystal). It also takes into account the density and location of the layer charge deficit (octahedral or tetrahedral) and the nature of the interlayer cation. As it is based on the exchange convention, this model makes it possible to reproduce quantitatively cation exchange reactions. It was validated against a variety of experimental datasets, including desorption isotherms of two saponites and two hectorites with contrasting layer charges and of Wyoming montmorillonite (SWy-1) with various interlayer compositions (Na and Ca). The present model is satisfactory from a phenomenological point of view as water is presumed to have a specific affinity for each cation and is not considered as an independent parameter, as in many alternative models. Finally, the hydrated exchange models were compared to the classic exchange approach, which conventionally involves anhydrous reactions, and data extracted from experiments involving clay in contact with saline solutions.

2. MATERIALS AND METHODS

2.1. Background

A hydrated smectite powder has three different water "reservoirs" (e.g. see Fig. 1 in Gailhanou et al., 2017).

The main one is the interlayer space, where water molecules are hydrating interlayer cations to different degrees (i.e. hydration sphere) according to layer charge, nature of interlayer cation, temperature, and relative humidity (e.g. Dazas et al., 2015). The other two reservoirs are the "external water", distributed across the external surfaces of clay tactoids (composed of a variable number of stacked layers) (Salles, 2006), and the pore water, located between the clay aggregates (built of connected clay tactoids). Pore water was not accounted for in the present study owing to its negligible role in clay swelling. Moreover, the distinction between interlayer and external water was not made in the present study. Indeed, only interlayer water was required to reproduce water isotherms up to a relative humidity of ~60–70%, in agreement with previous X-ray diffraction, neutron diffraction, and molecular modelling studies (Ferrage et al., 2005a, 2010, 2011; Vinci et al., 2020). A low contribution of external water in such conditions was also supported by Lindholm et al. (2019). Its contribution is only significant in the relative humidity range where pore water is also present.

2.2. Hydrated exchange reactions

The geochemical selectivity constant that relates the amount of a given species in solution with those adsorbed on the solid depends on the water content of the studied material (e.g. Redinha and Kitchener, 1963; Steck and Yeager, 1980). Regarding clay minerals, Tardy and Duplay (1992) included water molecules in the Na/Ca exchange reaction. Similarly, Whittaker et al. (2019) have proposed a Na/K exchange model in which the number of water planes was correlated to water activity. To take into account this effect, the Gapon convention (Gapon, 1933) was used here to model the ion exchange reactions involving water molecules in the interlayer space. This convention expresses exchange reaction per mol of exchange sites rather than per mol of exchanging ion (Gaines and Thomas, 1953). For monovalent Na^+ and bivalent Ca^{2+} cations, the reaction is thus written in the following way:

$$\mathrm{X}Na + 0.5Ca^{2+} \leftrightarrow Na^+ + \mathrm{X}Ca_{0.5} \quad (1)$$

where X^- represents the exchanger to which Na^+ or Ca^{2+} cation is bound.

The distribution of species is given by the law of mass action:

$$K_{Na/Ca} = \frac{E_{XCa_{0.5}}}{E_{XNa}} \times \frac{[Na^+]}{[Ca^{2+}]^{0.5}} \quad (2)$$

where $K_{Na/Ca}$ is the selectivity constant of the reaction (1), E referring to the equivalent fraction of species on the exchanger and brackets referring to the activity of Na^+ or Ca^{2+} in solution.

In the following, hydration reactions were defined in reference to the dry state. Hydration reactions involving Na^+ then write:

$$XNa + nH_2O \leftrightarrow XNa(H_2O)_n \quad (3)$$

where n is the number of water molecules in the interlayer space per layer charge (X).

For bivalent cations such as Ca^{2+}, the hydration reactions are written as follows:

$$XCa_{0.5} + nH_2O \leftrightarrow \mathrm{X}Ca_{0.5}(H_2O)_n \quad (4)$$

Following the Gapon convention, the general expression of mass action laws for hydration reactions is:

$$K_W = \frac{E_{XCation(H_2O)_n}}{E_{XCation}} \times \frac{1}{[H_2O]^n} \quad (5)$$

where K_w is the thermodynamic constant of the hydration reaction Eqs. (3)–(4) and $XCation$ refers to XNa (Eq. (3)) or $XCa_{0.5}$ (Eq. (4)).

The definition of Eqs. (3)–(5) illustrates interactions between water, the clay layer and interlayer cation. If necessary, the previous equation (Eq. (5)) can be modified according to the Rothmund-Kornfeld description (Bond, 1995):

$$K_W = \frac{E_{XCation(H_2O)_n}}{E_{XCation}} \times \left(\frac{1}{[H_2O]}\right)^{\beta} \quad (6)$$

where β is an empirical parameter. Note that Gapon and Rothmund-Kornfeld approaches are equivalent for $\beta = n$.

2.3. Modelling strategy

The calculations were performed with PHREEQC3 (Parkhurst and Appelo, 2013) and the thermodynamic database THERMOCHIMIE version 9a (Giffaut et al., 2014; Blanc et al., 2015). The simulation of water vapor sorption isotherms required the definition of pore water since the involved chemical reactions do not occur nor can be described in the absence of solvent. The cation concentration in pore water was set at 1 meq L^{-1} (i.e. solutions containing NaCl, $CaCl_2$ or NaCl/$CaCl_2$, with Cl concentration = 1 mmol L^{-1}). The salinity of the pore water was then adjusted by imposing a partial pressure of $H_2O(g)$ to control water activity. In addition, for a solution containing both Na^+ and Ca^{2+} aqueous species, the increase in the ionic strength of the solution modifies the cationic composition of the exchanger (e.g. Appelo and Postma, 2004; Fletcher and Sposito, 1989). To overcome this effect and reach conditions expected for water adsorption/desorption experiments, an extremely low quantity of pore water can be set in the system (i.e. < 0.1 g H_2O for 1 g of clay). In doing so, the quantity of cations present outside the smectite is much smaller than inside the interlayer spaces and the effect of salinity on the cationic composition of the exchanger can thus be disregarded. The initial Na^+/Ca^{2+} interlayer population is then independent of relative humidity, as expected during measurements of water vapor sorption isotherms. Furthermore, as the water activity is set in the models [set partial pressure of $H_2O(g)$] and the effect of salinity on exchangeable cations can be disregarded, simulations of water vapor isotherms do not require the use of activity coefficient corrections dedicated to high salinities, such as the Pitzer equations and their associated databases (e.g. Lach et al., 2018; Lassin et al., 2018).

2.4. Data selection

The water contents obtained along the adsorption branch of the isotherms are systematically lower than those measured during desorption (e.g. Bérend et al., 1995; Cases et al., 1992; Ferrage et al., 2010; Lindholm et al., 2019), as the result of various and complex processes (e.g. Woodruff and Revil, 2011) that disfavor water uptake. In the macroscopic approach proposed here, this could be addressed by using an energetic barrier corresponding to the energy required to re-expand the layer-to-layer distance. In addition, clay hydration along the desorption branch of the isotherms appears to be more homogeneous compared to the sorption branch (e.g. Bérend et al., 1995). Consequently, simulations focused on desorption branch of the isotherms for which no energetic barrier is involved.

Water desorption data of three different smectite minerals (saponite, hectorite, and montmorillonite) were taken from the literature. They were selected based on (i) the purity of investigated samples, (ii) data quality, and (iii) availability of results from complementary methods (e.g. X-ray diffraction) that allowed quantifying the relative proportion of the different hydration states. For saponite, data from Ferrage et al. (2010) were used. This study provides data for two samples containing interlayer Na and differing in their tetrahedral charge [0.8 and 1.4 charge equivalent per $O_{20}(OH)_4$]. These two samples are hereafter referred to as S-$Na_{0.8}$ and S-$Na_{1.4}$, respectively. For hectorite, we used data from Vinci et al. (2020). These authors studied the hydration of several sodium hectorites having octahedral charges ranging from 0.8 (hereinafter referred to as H-$Na_{0.8}$) to 1.6 (hereinafter referred to as H-$Na_{1.6}$) equivalent per $O_{20}(OH)_4$. Finally, for montmorillonite, the Wyoming montmorillonite (SWy-1) with a charge deficit of 0.74 equivalent per $O_{20}(OH)_4$ (e.g. Cases et al., 1992), mainly located in the octahedral sheet (e.g. Sato et al., 1992), was selected. The SWy-1 was used to study the effect of the interlayer cation nature (Na, Ca, and mixed Na/Ca) on water desorption isotherms. For this natural sample, changes of hydration state (e.g. from 2 W to 1 W) are less marked than those observed with synthetic materials listed above, possibly as the result of an increased surface charge heterogeneity compared to synthetic saponites and hectorites. Up to 3 water layers (3 W) have been identified at highest relative humidities for hectorite (Vinci et al., 2020) and montmorillonite (Cases et al., 1992; Holmboe et al., 2012). Dazas et al. (2014) showed that the 3 W layer cannot be described as 3 perfectly discrete planes, but that part ot its interlayer water has some characteristics of the bulk water. Overall, we assumed that the 3 W layer is involved in the crystalline swelling rather the osmotic swelling (e.g. Madsen and Müller-Vonmoos, 1989; Norrish, 1954) and therefore, we considered it in our modelling exercise.

3. RESULTS

3.1. Effect of smectite tetrahedral layer charge (saponite)

The total amount of water incorporated in S-$Na_{0.8}$ as a function of relative humidity (Fig. 1a) and the corresponding relative proportions of the different hydration states (Fig. 1b), extracted from Ferrage et al. (2010), show that the total interlayer water content is correlated to the variation in the proportions of 0 W, 1 W and 2 W interlayer hydration states.

S-$Na_{0.8}$ data were reproduced using the reactions and selectivity constants listed in Table 1. It was assumed that the species corresponding to 0 water layers did not involve water molecules (XNa in Table 1), although water molecules bound to the interlayer cation likely persist even at

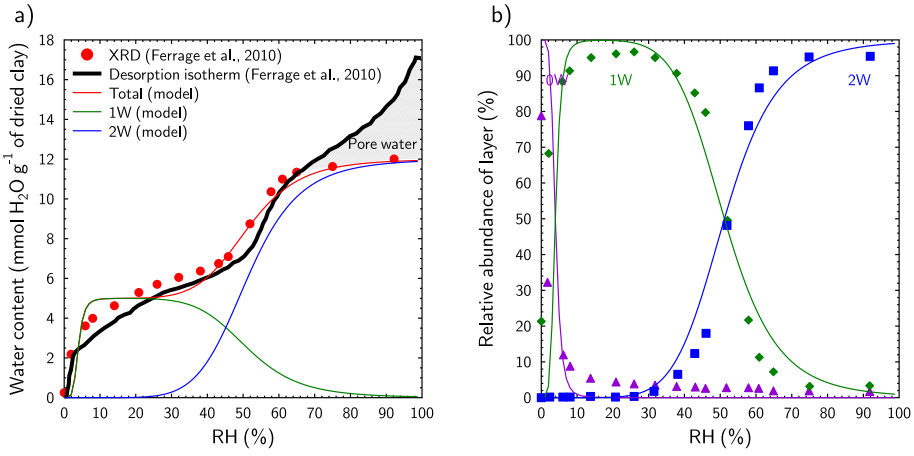

Fig. 1. (a) Comparison of water contents derived from modelling of the XRD profile (red circles) with those determined from the water vapor desorption isotherms (black curve). Taken from Ferrage et al. (2010) for the saponite S-$Na_{0.8}$. The green and blue curves indicate the quantity of water modelled for 1 and 2 layers (1 W and 2 W, repectively). The red curve represents the total quantity of water modelled (Total = 1 W + 2 W). (b) Evolution of the relative contribution of the different types of layers (0 W, 1 W and 2 W) as a function of relative humidity for the saponite S-$Na_{0.8}$. Symbols: experimental data from Ferrage et al. (2010). Curves: numerical results. Purple, green, and blue colors are respectively used for 0 W, 1 W, and 2 W. (For interpretation of the references to colour in this figure legend, the reader is referred to the web version of this article.)

Table 1
Reactions and selectivity constants used to simulate the dehydration of S-$Na_{0.8}$ and S-$Na_{1.4}$. For 1 g of S-$Na_{0.8}$, a charge deficit of 0.8 eq mol^{-1} and a molar mass of 776 g mol^{-1} (Ferrage et al., 2010), the exchanger quantity is 10^{-3} mol. For 1 g of S-$Na_{1.4}$, a charge deficit of 1.4 eq mol^{-1} and a molar mass of 789 g mol^{-1} (Ferrage et al., 2010), the exchanger quantity is 1.8 10^{-3} mol.

Clay	Reaction	Thermodynamic constant (log K_W)	Description
S-$Na_{0.8}$	$XNa + 5H_2O = XNa(H_2O)_5$	7	Exchange reaction involving 1 water layer (1 W)
	$XNa + 12H_2O = XNa(H_2O)_{12}$	9	Exchange reaction involving 2 water layers (2 W)
S-$Na_{1.4}$	$XNa + 2.8H_2O = XNa(H_2O)_{2.8}$	6.3	Exchange reaction involving 1 water layer (1 W)
	$XNa + 6.7H_2O = XNa(H_2O)_{6.7}$	8	Exchange reaction involving 2 water layers (2 W)

the lowest relative humidity (e.g. Cases et al., 1992; Kloprogge et al., 1992; Bérend et al., 1995; Rinnert et al., 2005).

The quantity of water in the 1 W (Table 1) was estimated to 5 10^{-3} mol H_2O g^{-1} of clay, using the Fig. 7 in Ferrage et al. (2010). Interestingly, this value is independent of the cation exchange capacity (CEC), an observation supported by Dazas et al. (2015). Consequently, the amount of water to be considered in hydration reaction (Eq. (3)) was corrected by the total exchangeable quantity following:

$$n_{1W} = \frac{5\ 10^{-3} \times m_{clay}}{n_{XNa}} \quad (7)$$

where m_{clay} is the clay mass considered in the numerical simulation and n_{XNa} is the corresponding exchanger quantity (in moles).

For 1 g of clay, a charge deficit of 0.8 equivalent per mole of clay and a molar mass of 776 g mol^{-1} (Ferrage et al., 2010), the exchanger quantity is 10^{-3} mol and one obtain $n_{1W} = 5$.

Likewise, for 2 water layers (2 W in Table 1), we found:

$$n_{2W} = \frac{12\ 10^{-3} \times m_{clay}}{n_{XNa}} = 12 \quad (8)$$

Overall, amounts of water calculated for 1 W and 2 W reactions agree with several works, including molecular modelling techniques (e.g. Ferrage et al., 2011; Dazas et al., 2014; Holmboe and Bourg, 2014). Both the desorption isotherm of Ferrage et al. (2010) and the relative contribution of the different types of layers were satisfyingly modelled (Fig. 1) with these parameters and refined selectivity constants (Table 1 and electronic annex S-Na0.8.pqi). The misfit at the highest relative humidity (grey area in Fig. 1a) in the desorption isotherm was due to the presence of pore water (Ferrage et al., 2010; Salles et al., 2013) which was not considered in this study.

Parameters and selectivity coefficients describing the hydration reaction of S-$Na_{1.4}$ were determined as for S-$Na_{0.8}$ and are shown in Table 1. Selectivity constants required further adjustment owing to the change in the number of water molecules involved in the hydration reactions (Eq. (3)). As for S-$Na_{0.8}$, both the desorption isotherms (Fig. 2a) and the relative contribution of the

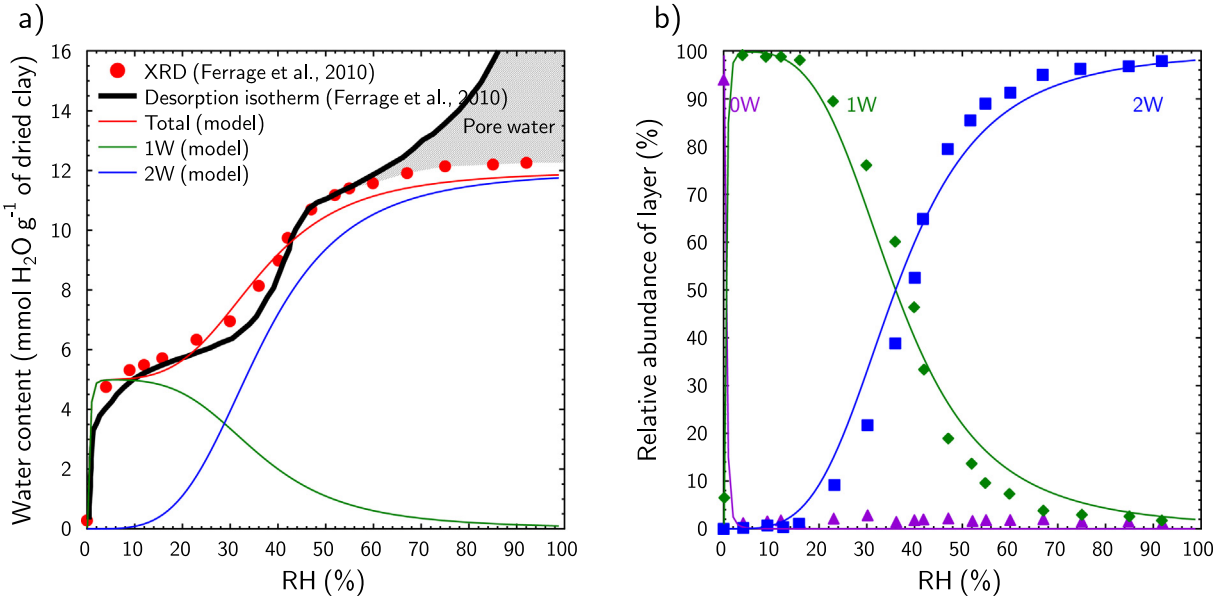

Fig. 2. (a) Comparison of water contents derived from modelling of the XRD profile (red circles) with those determined from the water vapor desorption isotherms (black curve). Taken from Ferrage et al. (2010) for the saponite S-$Na_{1.4}$. The green and blue curves indicate the quantity of water modelled for 1 and 2 layers (1 W and 2 W, repectively). The red curve represents the total quantity of water modelled (Total = 1 W + 2 W) b) evolution of the relative contribution of the different types of layers (0 W, 1 W and 2 W) as a function of relative humidity for the saponite S-$Na_{1.4}$. Symbols: experimental data from Ferrage et al. (2010). Curves: numerical results. Same color coding as in Fig. 1. (For interpretation of the references to colour in this figure legend, the reader is referred to the web version of this article.)

different types of layers (0 W, 1 W and 2 W - Fig. 2b) as a function of relative humidity quantitatively reproduced the experimental data of Ferrage et al. (2010). Our modelling accounted also for the observed broadening of the transition zone between 1 W and 2 W hydration states, which was due to a decrease of the exponents involved in mass action equations (2.8 and 6.7 for 1 W and 2 W reactions, respectively – see Eq. (5) and Table 1). Together with the data from S-$Na_{0.8}$, this successful data modelling showed that Gapon approach can model and predict Na-saponite hydration.

3.2. Effect of smectite octahedral layer charge (hectorite)

In sodium hectorite, and in contrast to saponite, the relative contributions of 0 W, 1 W, 2 W and 3 W as a function of relative humidity are independent of amount of layer charge (Vinci et al., 2020). As a consequence, hydration reactions must make use of equal exponents for water in the mass action equations independent of layer charge, and the Rothmund-Kornfeld description (Bond, 1995) is probably the most straightforward for this purpose. The parameters were constant whatever the layer charge (Table 2) and allowed us to reproduce the experimental desorption isotherms and the contributions of 0 W, 1 W, 2 W, and 3 W for both H-$Na_{0.8}$ and H-$Na_{1.6}$ (Fig. 3). An example of PHREEQC input file is given in Electronic Annex (see H-Na0.8.pqi). Note that the 3 W contribution was significant only at high relative humidity, where the contribution of pore water was also strong. Fitted parameters for hydration reaction involving 3 W layers are thus fraught with significant uncertainty.

3.3. Effect of the type of interlayer cation (SWy-1 smectite)

Experimental desorption isotherms of the Na-exchanged SWy-1, hereafter referred to as Na-SWy-1 (Fig. 4a – Cases et al. (1992), Bérend et al. (1995)), were successfully modelled using the Rothmund-Kornfeld parameters listed in Table 3. These values allowed also reproducing the experimentally derived relative contributions of 0 W, 1 W, 2 W, and 3 W layers (Fig. 4b). The water contents in 1 W and 2 W layers were estimated from the desorption isotherms. 3 W layers were also considered in the modelling of the high relative humidity (Fig. 4b), consistent with the reports of Holmboe et al. (2012) and Cases et al. (1992). As for hectorite, parameters refined for exchange reactions involving 3 W layers were poorly constrained owing to the overlap with the pore water contribution (Fig. 4a).

The same modelling procedure was applied to the experimental water desorption isotherm obtained for Ca-exchanged SWy-1 (Cases et al., 1997), hereafter referred to as Ca-SWy-1. As for Na-SWy-1, and although the plateaus in the desorption isotherms were less marked, a satisfying data modelling (with parameters listed in Table 3) could be obtained, both for the water desorption isotherm (Fig. 5a) and for the evolution of the relative number of 0 W, 1 W, 2 W, and 3 W layers (Fig. 5b). Overall, refined parameters (selectivity constants, Rothmund-Kornfeld coefficients, water contents for 1 W, 2 W, and 3 W) differed significantly from that established for Na-SWy-1 (Table 3) due to the hydration behavior of Ca-SWy-1. In contrast to its Na-exchanged counterpart, 2 W hydrates prevailed over a large range of relative humidity conditions in Ca-SWy-1.

4. DISCUSSION

A dependency on charge location was implemented here in the formalism used here to describe and model hydration reactions. The Gapon formalism was able to predict saponite hydration (S-$Na_{0.8}$ and S-$Na_{1.4}$), for which the clay layer and interlayer Na^+, and associated H_2O molecules, are strongly bound owing to the strong undersaturation of layer surface oxygen atoms (i.e. tetrahedral charge, Skipper et al., 1990; Prost et al., 1998; Michot et al., 2005). Further investigations are required however to assess the validity of this model for other cations (e.g. calcium saponite). The Rothmund-Kornfeld description was used for the modelling of hectorite and montmorillonite hydration (H-$Na_{0.8}$, H-$Na_{1.6}$, Na-SWy-1 and Ca-SWy-1), for

Table 2
Reactions and selectivity constants used to simulate the dehydration of H-$Na_{0.8}$ and H-$Na_{1.6}$. For 1 g of H-$Na_{0.8}$, a charge deficit of 0.8 eq mol^{-1} and a molar mass of 763 g mol^{-1}, the exchanger quantity is 10^{-3} mol. For 1 g of H-$Na_{1.6}$, a charge deficit of 1.6 eq mol^{-1} and a molar mass of 768 g mol^{-1}, the exchanger quantity is 2 10^{-3} mol.

Clay	Reaction	Thermodynamic constant (log K_W)	Rothmund-Kornfeld coefficient (β)	Description
H-$Na_{0.8}$	$XNa + 5.2H_2O = XNa(H_2O)_{5.2}$	4	3	Exchange reaction involving 1 water layer (1 W)
	$XNa + 12H_2O = XNa(H_2O)_{12}$	7	13.2	Exchange reaction involving 2 water layers (2 W)
	$XNa + 18H_2O = XNa(H_2O)_{18}$	6.7	50	Exchange reaction involving 3 water layers (3 W)
H-$Na_{1.6}$	$XNa + 2.6H_2O = XNa(H_2O)_{2.6}$	4	3	Exchange reaction involving 1 water layer (1 W)
	$XNa + 6H_2O = XNa(H_2O)_6$	7	13.2	Exchange reaction involving 2 water layers (2 W)
	$XNa + 9H_2O = XNa(H_2O)_9$	6.7	50	Exchange reaction involving 3 water layers (3 W)

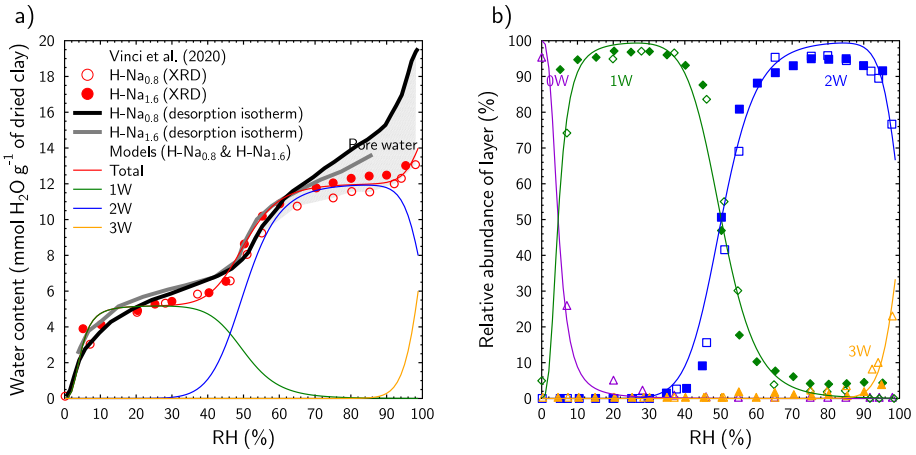

Fig. 3. (a) Comparison of water contents derived from modelling of the XRD profile (red circles) with those determined from the water vapor desorption isotherms (black and grey curves). Taken from Vinci et al. (2020) for hectorites H-$Na_{0.8}$ and H-$Na_{1.6}$. The green, blue and orange curves indicate the quantity of water modelled for 1, 2 and 3 layers (1 W, 2 W and 3 W, respectively) for both H-$Na_{0.8}$ and H-$Na_{1.6}$. The red curve represents the total quantity of water modelled (Total = 1 W + 2 W + 3 W) for both H-$Na_{0.8}$ and H-$Na_{1.6}$. (b) Evolution of the relative contribution of the different types of layers (0 W, 1 W, 2 W and 3 W) as a function of relative humidity. Open and fill symbols: experimental data from Vinci et al. (2020) for H-$Na_{0.8}$ and H-$Na_{1.6}$, respectively. Curves: numerical results. Purple, green, blue and yellow colors are respectively used for 0 W, 1 W, 2 W and 3 W. (For interpretation of the references to colour in this figure legend, the reader is referred to the web version of this article.)

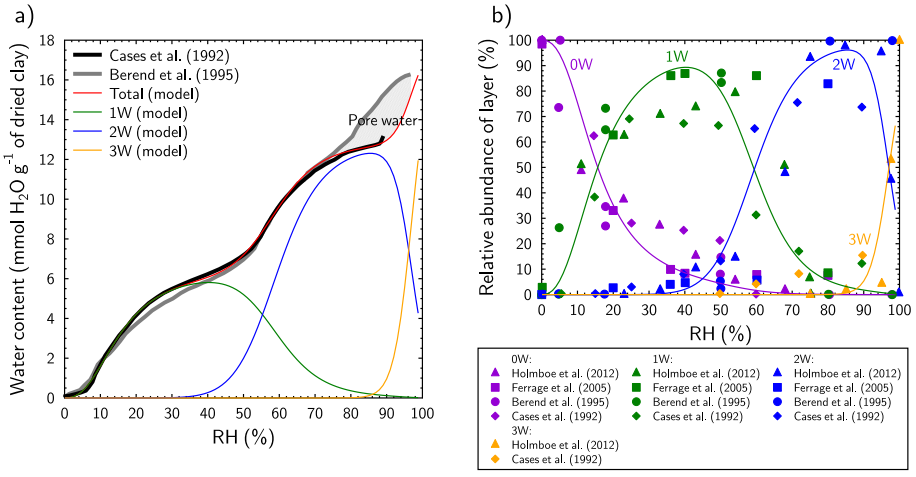

Fig. 4. (a) Desorption isotherm obtained for the smectite Na-SWy-1. (b) Evolution of the relative contribution of the different types of layers (0 W, 1 W, 2 W and 3 W) as a function of relative humidity for the smectite Na-SWy-1. Same color coding as in Fig. 3.

Table 3
Reactions and selectivity constants used to simulate the dehydration of Na-SWy-1 and Ca-SWy-1. For 1 g of clay, a charge deficit of 0.74 eq mol^{-1} and a molar mass of 742 g mol^{-1} (Cases et al., 1992), the exchanger quantity is 10^{-3} mol.

Clay	Reaction	Thermodynamic constant (log K_W)	Rothmund-Kornfeld coefficient (β)	Description
Na-SWy-1	$XNa + 6.5H_2O = XNa(H_2O)_{6.5}$	2	2.5	Exchange reaction involving 1 water layer (1 W)
	$XNa + 12.8H_2O = XNa(H_2O)_{12.8}$	4.1	12	Exchange reaction involving 2 water layers (2 W)
	$XNa + 18H_2O = XNa(H_2O)_{18}$	4.4	50	Exchange reaction involving 3 water layers (3 W)
Ca-SWy-1	$XCa_{0.5} + 4H_2O = XCa_{0.5}(H_2O)_4$	7.3	5.5	Exchange reaction involving 1 water layer (1 W)
	$XCa_{0.5} + 12.9H_2O = XCa_{0.5}(H_2O)_{12.9}$	8.78		Exchange reaction involving 2 water layers (2 W)
	$XCa_{0.5} + 16H_2O = XCa_{0.5}(H_2O)_{16}$	950		Exchange reaction involving 3 water layers (3 W)

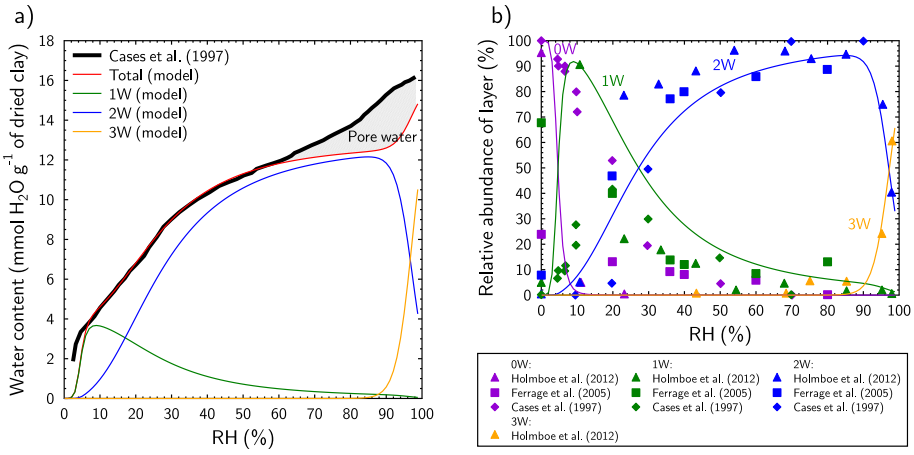

Fig. 5. (a) Desorption isotherm obtained for the smectite Ca-SWy-1. (b) Evolution of the relative contribution of the different types of layers (0 W, 1 W, 2 W and 3 W) as a function of relative humidity for the smectite Ca-SWy-1. Same color coding as in Fig. 3.

which water molecules interact weakly with the clay layer (i.e. octahedral charge, Doner and Mortland, 1971; Prost et al., 1998; Vinci et al., 2020). The later empirical description may also be used to describe saponite hydration, however, as both Gapon and Rothmund-Kornfeld approaches are equivalent when $\beta = n$ (Eq. (5)–(6)). Regarding ion exchange reactions, the Rothmund-Kornfeld description has been found to be applicable in numerous cases (e.g. Bond and Verburg, 1997; Escudey et al., 2001; Reynolds and Tardiff, 2015). As reported by Bond (1995), it appears more accurate because it avoids extrapolation of the data required for the thermodynamic approach.

The capacity of our model to predict the complex hydration behavior of clays exposed to contrasting environmental conditions was evaluated for a smectite interacting with a mixed cation pore water composition using parameters previously established for Na-SWy-1 and Ca-SWy-1 (Table 3). The desorption isotherm calculated for the clay SWy-1 with ~50% of Na^+ and ~25% of Ca^{2+} (i.e. $\Sigma XCa_{0.5}(H_2O)_n \sim 50\%$) is shown in Fig. 6a (green curve). The PHREEQC input file is given in Electronic Annex (see SWy-1_NaCa.pqi). This isotherm was calculated as a simple weighted sum of water layer contributions from Na and Ca end-members. Such an assumption relies on the presence of homoionic interlayers and is supported by numerous works showing a segregation of cations in different interlayers (e.g. Méring and Glaeser, 1954; Ferrage et al., 2005c; Möller et al., 2010). Nonetheless, cation demixing is a complex phenomenon that depends on several parameters such as the substitution level (Fink et al., 1971) or the layer charge (Laird, 2006). The desorption isotherm of the smectite Na/Ca-SWy-1 was then found in

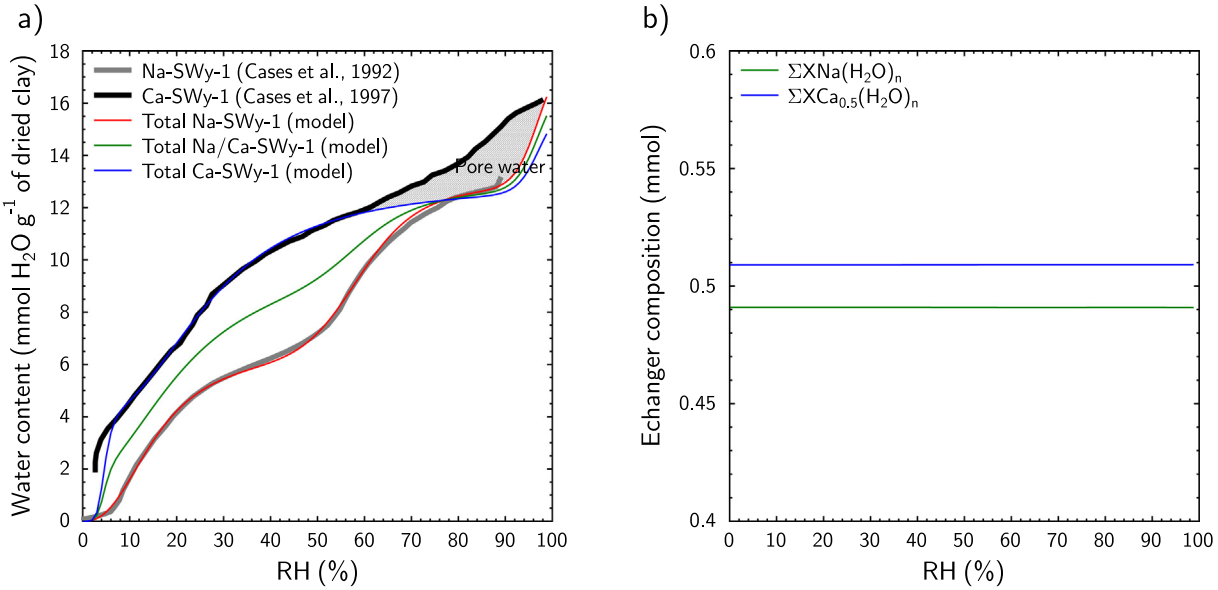

Fig. 6. (a) Desorption isotherms obtained for the smectites Na-SWy-1, Ca-SWy-1 and Na/Ca-SWy-1. (b) Exchanger composition as a function of relative humidity for the smectite Na/Ca-SWy-1 (calculation performed without pore water, see text).

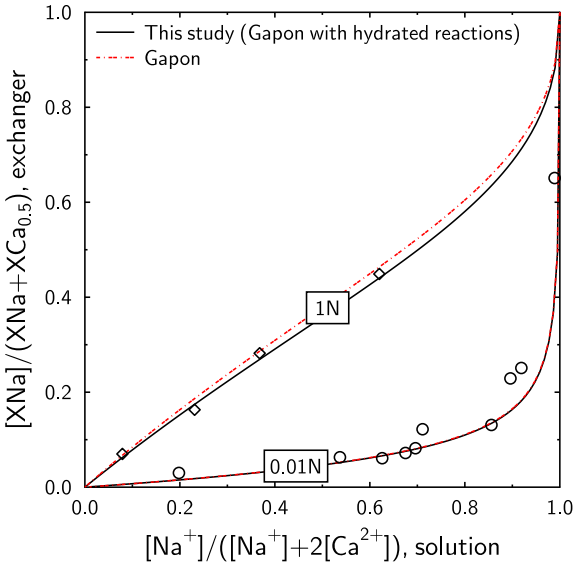

Fig. 7. Comparison of Na/Ca exchange isotherms obtained using anhydrous and hydrated reactions for total Na and Ca concentrations (i.e. [Na] + [Ca]) from 0.01 to 1 mol L^{-1}. The open circles and diamonds refer to the experimental data obtained by Tang and Sparks (1993) and Amrhein and Suarez (1991) for the smectite SWy-1 at 0.01 and 1 mol L^{-1}, respectively.

between that of the smectite Na-SWy-1 (red curve) and that of Ca-SWy-1 (blue curve). A similar behavior has been observed by Keren and Shainberg (1979) on the adsorption isotherm of a mixed Na/Ca Wyoming. Consistent with the adopted simulation approach (see Section 2.3), and as expected during an isotherm measurement, the proportion of Na and Ca in the interlayer space was independent of relative humidity (Fig. 6b).

The proposed model allowed also predicting the effect of solution salinity on the interlayer composition of the SWy-1 (Fig. 7). In accordance with the cation exchange data of Gaucher et al. (2009), the selectivity constant of the anhydrous Na/Ca exchange reaction (Eq. (1)) was equal to 0.35 (log unit). At lowest salinities, the presence of most hydrated species (i.e. 3 W hydration reactions reported in Table 3) were expected from previous considerations, however, and thermodynamic exchange constant must be corrected when Eq. (1) is coupled with Eqs. (3)–(4):

$$LogK_{Na/Ca}^{hydrated} = LogK_{3W}^{Na-SWy-1} - LogK_{3W}^{Ca-SWy-1} + LogK_{Na/Ca}^{anhydrous} \quad (9)$$

where $K_{Na/Ca}^{hydrated}$ is the selectivity constant for hydrated Na/Ca exchange reaction, $K_{3W}^{Na-SWy-1}$ the thermodynamic constant of the 3 W hydration reaction involving the Na-SWy-1 (Table 3), $K_{3W}^{Ca-SWy-1}$ the thermodynamic constant of the 3 W hydration reaction involving the Ca-SWy-1 (Table 3) and $K_{Na/Ca}^{anhydrous}$ the selectivity constant of the anhydrous Na/Ca exchange reaction ($10^{0.35}$).

The Na/Ca exchange isotherm has been calculated for total Na and Ca concentrations of 0.01 and 1 mol L^{-1} (Cl^- as charge-compensating anion). As showed in numerous studies (e.g. Fletcher and Sposito, 1989; Appelo and Postma, 2004), calculations depend on the exponent used in the mass action equation (Eq. (2)) and thus the content of adsorbed Ca^{2+} increases with the decrease of the ionic strength. The exchange isotherms obtained with the Gapon convention involving anhydrous and hydrated reactions (Eq. (1) vs. Eq. (1), (3)–(4)) overlapped for 0.01 mol L^{-1} concentrations (Fig. 7), whereas a minor effect of salinity on the apparent selectivity coefficient was observed for 1 mol L^{-1} concentrations, which is the validity limit of the B-dot activity model (Trémosa et al., 2014). Such discrepancy was due to the non-parallel evolution in water layer contributions from Na and Ca end-members with increasing ionic strength; as cation exchange and hydration reactions are coupled, clay hydration state affects in turn the exchange reaction through a feedback effect. This is supported by several works (e.g. Laird and Shang, 1997; Van Loon and Glaus, 2008; Whittaker et al., 2019). Note that a concentration of 1 mol L^{-1} is equivalent to 95.6 and 94.2% of relative humidity in NaCl and $CaCl_2$ type solutions, respectively. Salinity range investigated thus corresponded to the domain where a high contribution of 3 W was expected (Fig. 4 and Fig. 5). Despite 3 W reactions being weakly constrained (see Section 3.3), the exchange isotherms modelled at 0.01 and 1 mol L^{-1} reproduced the data, even for low salinity and high Na contents (Fig. 7). Moreover, at high ionic strengths, formation of $CaCl^+$ ionic pairs and their incorporation in the interlayer space should ideally be taken into account (Ferrage et al., 2005b; Tertre et al., 2011; Tournassat et al., 2011). As initial first approximation, the exchange of this complex was disregarded in our simulations.

5. IMPLICATIONS

The proposed approach does not require the thermodynamic properties of formation of the solids (i.e. clay layers) to be quantified, thus offering greater flexibility, and making it easier to include these models in complex, dynamic systems like soils and sediments. An issue hampering the inclusion of phyllosilicate hydration models in geochemical models resides in the fact that clays, and more especially smectite minerals, have exchangeable interlayer ions. These exchange reactions influence in turn clay hydration behavior (Bérend et al., 1995; Cases et al., 1997). Cation exchanges can be dealt with using non-ideal solid solutions including specific parameters such as Margules parameters (Pabalan, 1994), but most studies dealing with cationic exchange use simpler Gaines and Thomas (1953), Gapon (1933) or Vanselow (1932) formalisms, that involve fewer parameters. These models proved to be extremely robust and efficient for predicting cation migration in clay rocks (Tournassat et al., 2015). The developed approach to predict clay hydration is comparable to that established to quantify and predict cation exchanges in interlayer spaces and sorption on clay edges, which is known as 'surface complexation'. In addition, the developed model could be complemented with a surface complexation model to account for external water, based, for instance, on the work of Prost et al. (1998) and/or Lindholm et al. (2019). Such approach would allow refining water balance calculation

in reactive transport modelling and coupling more accurately the feedback of chemistry on flow. The importance of such a coupling has been discussed by Seigneur et al. (2018).

The coupling between hydration and exchange reactions could be also considered to study the evolution of apparent selectivity constants with the increase of the ionic strength (e.g. Liu et al., 2004). Finally, the hysteresis of water sorption onto clays (e.g. Cases et al., 1992) could be addressed using an energy barrier, the transition from a weakly hydrated species to a highly hydrated species (e.g. from 1 W to 2 W) then requiring more energy than the opposite reaction. The consideration of an energy barrier could be similar to what is done for a mineral precipitation beyond an over saturation window. In water-saturated conditions and in presence of different cations (e.g. Na^+ and K^+, the last one leading to weakly hydrated clay), this energy barrier could induce also an exchange hysteresis (Laird and Shang, 1997), that remains to be thoroughly investigated.

6. CONCLUSION

The proposed modelling approach allows reproducing satisfactorily experimentally derived water vapor desorption isotherms as well as the different clay hydration states for contrasting charge deficits located in both tetrahedral and octahedral positions. Mass action equations derived from the Gapon convention are well-suited to describe clay hydration involving strong interactions between water molecules and the clay layer (i.e. tetrahedral charge). In contrast, the Rothmund-Kornfeld description may be used whatever the location of the layer charge deficit (tetrahedral or octahedral).

The proposed approach, based on an exchange model, is very easy to implement in geochemical codes and is satisfactory from a phenomenological point of view. Consistent with XRD characterizations of water vapor sorption isotherms, most of water molecules are found in smectite interlayer, whereas the relative proportions of the different smectite hydration states depend on both interlayer composition and relative humidity. The consideration of hydration reactions for the Wyoming smectite does not indicate significant change on Na/Ca cation exchange within the concentration range studied (i.e. <1 mol L^{-1}) but further work is required to extend the model to other cations (K^+, Mg^{2+}, Sr^{2+} etc.). In addition, this approach, by distinguishing explicitly the hydration/cation exchange process from the thermodynamic stability of the clay layer, is compatible with the use of reaction kinetics. In the long term, the method put forward here should allow linking chemistry to water content in soils, in clay rocks and mechanics that is swelling pressures.

Declaration of Competing Interest

The authors declare that they have no known competing financial interests or personal relationships that could have appeared to influence the work reported in this paper.

ACKNOWLEDGMENTS

The authors thank C. Tournassat for fruitful discussions, Carl I. Steefel for editorial handling and the anonymous reviewers for their constructive remarks. BRGM contributors acknowledge funding by internal research grants (HyDoLa and THERMO-DDEM projects). ISTerre is part of Labex OSUG@2020 (ANR10 LABX56). BL thanks the CNRS interdisciplinary research program Needs, through its "MiPor" project, for financial support.

APPENDIX A. SUPPLEMENTARY MATERIAL

Supplementary data to this article can be found online at https://doi.org/10.1016/j.gca.2020.05.029.

REFERENCES

Amrhein C. and Suarez D. (1991) Sodium-calcium exchange with anion exclusion and weathering corrections. *Soil Sci. Soc. Am. J.* **55**, 698–706.

Appelo C. A. J. and Postma D. (2004) *Geochemistry, groundwater and pollution*. CRC Press.

Arthur E., Tuller M., Moldrup P. and Jonge L. W. D. (2016) Evaluation of theoretical and empirical water vapor sorption isotherm models for soils. *Water Resources Res.* **52**, 190–205.

Bérend I., Cases J. M., Francois M., Uriot J. P., Michot L., Masion A. and Thomas F. (1995) Mechanism of adsorption and desorption of water vapor by homoionic montmorillonites; 2, The Li+, Na+, K+, Rb+ and Cs+ - exchanged forms. *Clays Clay Miner.* **43**, 324–336.

Blanc P., Vieillard P., Gailhanou H., Gaboreau S., Marty N., Claret F., Madé B. and Giffaut E. (2015) ThermoChimie database developments in the framework of cement/clay interactions. *Appl. Geochem.* **55**, 95–107.

Bond W. J. (1995) On the Rothmund-Kornfeld description of cation exchange. *Soil Sci. Soc. Am. J.* **59**, 436–443.

Bond W. J. and Verburg K. (1997) Comparison of methods for predicting ternary exchange from binary isotherms. *Soil Sci. Soc. Am. J.* **61**, 444–454.

Bray H. J., Redfern S. A. T. and Clark S. M. (1998) The kinetics of dehydration in Ca-montmorillonite; an in situ X-ray diffraction study. *Mineral. Mag.* **62**, 647–656.

Cases J., Bérend I., François M., Uriot J., Michot L. and Thomas F. (1997) Mechanism of adsorption and desorption of water vapor by homoionic montmorillonite; 3, The Mg^{2+}, Ca^{2+}, and Ba^{3+} exchanged forms. *Clays Clay Miner.* **45**, 8–22.

Cases J. M., Berend I., Besson G., Francois M., Uriot J. P., Thomas F. and Poirier J. E. (1992) Mechanism of adsorption and desorption of water vapor by homoionic montmorillonite. 1. The sodium-exchanged form. *Langmuir* **8**, 2730–2739.

Cornelis W. M., Corluy J., Medina H., Díaz J., Hartmann R., Van Meirvenne M. and Ruiz M. E. (2006) Measuring and modelling the soil shrinkage characteristic curve. *Geoderma* **137**, 179–191.

Dazas B., Ferrage E., Delville A. and Lanson B. (2014) Interlayer structure model of tri-hydrated low-charge smectite by X-ray diffraction and Monte Carlo modeling in the Grand Canonical ensemble. *Am. Mineral.* **99**, 1724–1735.

Dazas B., Lanson B., Delville A., Robert J.-L., Komarneni S., Michot L. J. and Ferrage E. (2015) Influence of tetrahedral layer charge on the organization of interlayer water and ions in synthetic Na-saturated smectites. *J. Phys. Chem. C* **119**, 4158–4172.

Doner H. E. and Mortland M. M. (1971) Charge location as a factor in the dehydration of 2:1 clay minerals. *Soil Sci. Soc. Am. J.* **35**, 360–362.

Dubacq B., Vidal O. and De Andrade V. (2009) Dehydration of dioctahedral aluminous phyllosilicates: thermodynamic modelling and implications for thermobarometric estimates. *Contrib. Miner. Petrol.* **159**, 159.

Escudey M., Díaz P., Förster J. E., Pizarro C. and Galindo G. (2001) Gaines–thomas and rothmund–kornfeld descriptions of potassium–calcium exchange on variable surface charge soils. *Commun. Soil Sci. Plant Anal.* **32**, 3087–3097.

Ferrage E., Lanson B., Michot L. J. and Robert J.-L. (2010) Hydration properties and interlayer organization of water and ions in synthetic Na-smectite with tetrahedral layer charge. Part 1. Results from X-ray diffraction profile modeling. *J. Phys. Chem. C* **114**, 4515–4526.

Ferrage E., Lanson B., Sakharov B. A. and Drits V. A. (2005a) Investigation of smectite hydration properties by modeling experimental X-ray diffraction patterns. Part I. Montmorillonite hydration properties. *Am. Mineral.* **90**, 1358–1374.

Ferrage E., Sakharov B. A., Michot L. J., Delville A., Bauer A., Lanson B., Grangeon S., Frapper G., Jiménez-Ruiz M. and Cuello G. J. (2011) Hydration properties and interlayer organization of water and ions in synthetic Na-smectite with tetrahedral layer charge. Part 2. Toward a precise coupling between molecular simulations and diffraction data. *J. Phys. Chem. C* **115**, 1867–1881.

Ferrage E., Tournassat C., Rinnert E., Charlet L. and Lanson B. (2005b) Experimental evidence for Ca-chloride ion pairs in the interlayer of montmorillonite. An XRD profile modeling approach. *Clays Clay Miner.* **53**, 348–360.

Ferrage E., Tournassat C., Rinnert E. and Lanson B. (2005c) Influence of pH on the interlayer cationic composition and hydration state of Ca-montmorillonite: Analytical chemistry, chemical modelling and XRD profile modelling study. *Geochim. Cosmochim. Acta* **69**, 2797–2812.

Fink D. H., Nakayama F. S. and McNeal B. L. (1971) Demixing of exchangeable cations in free-swelling bentonite clay. *Soil Sci. Soc. Am. J.* **35**, 552–555.

Fletcher P. and Sposito G. (1989) Chemical modeling of clay/electrolyte interactions of montmorillonite. *Clay Miner.* **24**, 375–391.

Gailhanou H., Vieillard P., Blanc P., Lassin A., Denoyel R., Bloch E., De Weireld G., Gaboreau S., Fialips C. I., Madé B. and Giffaut E. (2017) Methodology for determining the thermodynamic properties of smectite hydration. *Appl. Geochem.* **82**, 146–163.

Gaines G. L. and Thomas H. C. (1953) Adsorption studies on clay minerals. II. A formulation of the thermodynamics of exchange adsorption. *J. Chem. Phys.* **21**(4), 714–718.

Gapon Y. N. (1933) On the theory of exchange adsorption in soils. *J. Gen. Chern. U.S.S.R. (Engl. Trans.)* **3**, 144–160.

Gaucher E. C., Tournassat C., Pearson F. J., Blanc P., Crouzet C., Lerouge C. and Altmann S. (2009) A robust model for pore-water chemistry of clayrock. *Geochim. Cosmochim. Acta* **73**, 6470–6487.

Giffaut E., Grivé M., Blanc P., Vieillard P., Colàs E., Gailhanou H., Gaboreau S., Marty N., Madé B. and Duro L. (2014) Andra thermodynamic database for performance assessment: ThermoChimie. *Appl. Geochem.* **49**, 225–236.

Griffin J. J., Windom H. and Goldberg E. D. (1968) The distribution of clay minerals in the World Ocean. *Deep Sea Res. Oceanographic Abst.* **15**, 433–459.

Guggenheim S., Adams J. M., Bain D. C., Bergaya F., Brigatti M. F., Drits V. A., Formoso M. L. L., Galan E., Kogure T. and Stanjek H. (2006) Summary of recommendations of nomenclature committees relevant to clay mineralogy: Report of the Association Internationale pour l'Etude des Argiles (AIPEA) Nomenclature. *Clays Clay Miner.* **54**, 761–772.

Hatch C. D., Wiese J. S., Crane C. C., Harris K. J., Kloss H. G. and Baltrusaitis J. (2012) Water adsorption on clay minerals as a function of relative humidity: application of BET and freundlich adsorption. *Models. Langmuir* **28**.

Holmboe M. and Bourg I. C. (2014) Molecular dynamics simulations of water and sodium diffusion in smectite interlayer nanopores as a function of pore size and temperature. *J. Phys. Chem. C* **118**, 1001–1013.

Holmboe M., Wold S. and Jonsson M. (2012) Porosity investigation of compacted bentonite using XRD profile modeling. *J. Contam. Hydrol.* **128**, 19–32.

Jackson M. L. (1957) Frequency distribution of clay minerals in major great soil groups as related to the factors of soil formation. *Clays Clay Miner.* **6**, 133–143.

Keren R. and Shainberg I. (1979) Water Vapor isotherms and heat of immersion of Na/Ca-Montmorillonite systems—II: mixed systems. *Clays Clay Miner.* **27**, 145–151.

Kloprogge J. T., Jansen J. B. H., Schuiling R. D. and Geus J. W. (1992) The interlayer collapse during dehydration of synthetic Na0. 7-beidellite: a 23Na solid-state magic-angle spinning NMR study. *Clays Clay Miner.* **40**, 561–566.

Lach A., André L., Guignot S., Christov C., Henocq P. and Lassin A. (2018) A pitzer parametrization to predict solution properties and salt solubility in the H-Na–K–Ca–Mg–NO_3–H_2O system at 298.15 K. *J. Chem. Eng. Data* **63**, 787–800.

Laird D. A. (2006) Influence of layer charge on swelling of smectites. *Appl. Clay Sci.* **34**, 74–87.

Laird D. A. and Shang C. (1997) Relationship between cation exchange selectivity and crystalline swelling in expanding 2:1 phyllosilicates. *Clays Clay Miner.* **45**, 681–689.

Lassin A., André L., Lach A., Thadée A.-L., Cézac P. and Serin J.-P. (2018) Solution properties and salt-solution equilibria in the H-Li-Na-K-Ca-Mg-Cl-H2O system at 25 °C: A new thermodynamic model based on Pitzer's equations. *Calphad* **61**, 126–139.

Lindholm J., Boily J.-F. and Holmboe M. (2019) Deconvolution of smectite hydration isotherms. *ACS Earth and Space Chem.*.

Liu C., Zachara J. M. and Smith S. C. (2004) A cation exchange model to describe Cs+ sorption at high ionic strength in subsurface sediments at Hanford site, USA. *J. Contam. Hydrol.* **68**, 217–238.

Madsen F. T. and Müller-Vonmoos M. (1989) The swelling behaviour of clays. *Appl. Clay Sci.* **4**, 143–156.

Marty N. C. M., Lach A., Lerouge C., Grangeon S., Claret F., Fauchet C., Madé B., Lundy M., Lagroix F., Tournassat C. and Tremosa J. (2018) Weathering of an argillaceous rock in the presence of atmospheric conditions: A flow-through experiment and modelling study. *Appl. Geochem.* **96**, 252–263.

Marty N. C. M., Munier I., Gaucher E. C., Tournassat C., Gaboreau S., Vong C. Q., Giffaut E., Cochepin B. and Claret F. (2014) Simulation of cement/clay interactions: feedback on the increasing complexity of modelling strategies. *Transp. Porous Media* **104**, 385–405.

Méring J. and Glaeser R. (1954) Sur le rôle de la valence des cations échangeables dans la montmorillonite. *Bull. Minér.*, 519–530.

Michot L. J., Bihannic I., Pelletier M., Rinnert E. and Robert J.-L. (2005) Hydration and swelling of synthetic Na-saponites: Influence of layer charge. *Am. Mineral.* **90**, 166–172.

Möller M. W., Hirsemann D., Haarmann F., Senker J. and Breu J. (2010) Facile scalable synthesis of rectorites. *Chem. Mater.* **22**, 186–196.

Murray H. H. and Leininger R. K. (1955) Effect of weathering on clay minerals. *Clays Clay Miner.* **4**, 340–347.

Norrish K. (1954) The swelling of montmorillonite. *Discuss. Faraday Soc.* **18**, 120–134.

Pabalan R. T. (1994) Thermodynamics of ion exchange between clinoptilolite and aqueous solutions of na+k+ and na+ca2+. *Geochim. Cosmochim. Acta* **58**, 4573–4590.

Parkhurst D. L. and Appelo C. (2013) Description of input and examples for PHREEQC version 3—a computer program for speciation, batch-reaction, one-dimensional transport, and inverse geochemical calculations. *US Geolog. Surv. Techn. Methods, Book* **6**, 497.

Prost R., Koutit T., Benchara A. and Huard E. (1998) State and location of water adsorbed on clay minerals; consequences of the hydration and swelling-shrinkage phenomena. *Clays Clay Miner.* **46**, 117–131.

Ransom B. and Helgeson H. C. (1994) A chemical and thermodynamic model of aluminous dioctahedral 2:1 layer clay minerals in diagenetic processes; regular solution representation of interlayer dehydration in smectite. *Am. J. Sci.* **294**, 449–484.

Rawls W. J., Gish T. J. and Brakensiek D. L. (1991) Estimating soil water retention from soil physical properties and characteristics. In *Advances in Soil Science*, Vol. 16 (ed. B. A. Stewart). Springer New York, New York, NY, pp. 213–234.

Redinha J. and Kitchener J. (1963) Thermodynamics of ion-exchange processes. System H, Na and Ag with polystyrene sulphonate resins. *Trans. Faraday Soc.* **59**, 515–529.

Revil A. and Lu N. (2013) Unified water isotherms for clayey porous materials. *Water Resour. Res.* **49**, 5685–5699.

Reynolds J. and Tardiff B. (2015) A Rothmund-Kornfeld model of Cs^+–K^+–Na^+ exchange on spherical resorcinol-formaldehyde (sRF) resin in Hanford nuclear waste. *J. Radioanal. Nucl. Chem.*.

Rinnert E., Carteret C., Humbert B., Fragneto-Cusani G., Ramsay J. D. F., Delville A., Robert J.-L., Bihannic I., Pelletier M. and Michot L. J. (2005) Hydration of a synthetic clay with tetrahedral charges: A multidisciplinary experimental and numerical study. *J. Phys. Chem. B* **109**, 23745–23759.

Rotenberg B., Marry V., Dufrêche J.-F., Malikova N., Giffaut E. and Turq P. (2007) Modelling water and ion diffusion in clays: A multiscale approach. *C. R. Chim.* **10**, 1108–1116.

Salles F. (2006) Hydration of swelling clays: multi-scale sequence of hydration and determination of macroscopic energies from microscopic properties. *Université Pierre et Marie Curie - Paris VI.*.

Salles F., Douillard J.-M., Bildstein O., Gaudin C., Prelot B., Zajac J. and Van Damme H. (2013) Driving force for the hydration of the swelling clays: Case of montmorillonites saturated with alkaline-earth cations. *J. Colloid Interface Sci.* **395**, 269–276.

Sato T., Watanabe T. and Otsuka R. (1992) Effects of layer charge, charge location, and energy change on expansion properties of dioctahedral smectites. *Clays Clay Miner.* **40**, 103–113.

Seigneur N., Lagneau V., Corvisier J. and Dauzères A. (2018) Recoupling flow and chemistry in variably saturated reactive transport modelling - An algorithm to accurately couple the feedback of chemistry on water consumption, variable porosity and flow. *Adv. Water Resour.* **122**, 355–366.

Skipper N. T., Soper A. K., McConnell J. D. C. and Refson K. (1990) The structure of interlayer water in a hydrated 2:1 clay. *Chem. Phys. Lett.* **166**, 141–145.

Steck A. and Yeager H. (1980) Water sorption and cation-exchange selectivity of a perfluorosulfonate ion-exchange polymer. *Anal. Chem.* **52**, 1215–1218.

Tajeddine L., Gailhanou H., Blanc P., Lassin A., Gaboreau S. and Vieillard P. (2015) Hydration–dehydration behavior and thermodynamics of MX-80 montmorillonite studied using thermal analysis. *Thermochim. Acta* **604**, 83–93.

Tang L. and Sparks D. L. (1993) Cation-exchange kinetics on montmorillonite using pressure-jump relaxation. *Soil Sci. Soc. Am. J.* **57**, 42–46.

Tardy Y. and Duplay J. (1992) A method of estimateng the Gibbs free energies of formation of hydrated and dehydrated clay minerals. *Geochim. Cosmochim. Acta* **56**, 3007–3029.

Tertre E., Prêt D. and Ferrage E. (2011) Influence of the ionic strength and solid/solution ratio on Ca(II)-for-Na+ exchange on montmorillonite. Part 1: Chemical measurements, thermodynamic modeling and potential implications for trace elements geochemistry. *J. Colloid Interface Sci.* **353**, 248–256.

Tournassat C., Bizi M., Braibant G. and Crouzet C. (2011) Influence of montmorillonite tactoid size on Na–Ca cation exchange reactions. *J. Colloid Interface Sci.* **364**, 443–454.

Tournassat C., Steefel C. I., Bourg I. C. and Bergaya F. (2015) *Natural and engineered clay barriers*. Elsevier.

Trémosa J., Castillo C., Vong C. Q., Kervévan C., Lassin A. and Audigane P. (2014) Long-term assessment of geochemical reactivity of CO2 storage in highly saline aquifers: Application to Ketzin, In Salah and Snøhvit storage sites. *Int. J. Greenhouse Gas Control* **20**, 2–26.

Tremosa J., Gailhanou H., Chiaberge C., Castilla R., Gaucher E. C., Lassin A., Gout C., Fialips C. and Claret F. (2020) Effects of smectite dehydration and illitisation on overpressures in sedimentary basins: A coupled chemical and thermo-hydro-mechanical modelling approach. *Mar. Pet. Geol.* **111**, 166–178.

Van Loon L. R. and Glaus M. A. (2008) Mechanical compaction of smectite clays increases ion exchange selectivity for cesium. *Environ. Sci. Technol.* **42**, 1600–1604.

Vanselow A. P. (1932) Equilibria of the base-exchange reactions of bentonites, permutites, soil colloids, and zeolites. *Soil Sci.* **33**, 95–114.

Vidal O. and Dubacq B. (2009) Thermodynamic modelling of clay dehydration, stability and compositional evolution with temperature, pressure and H2O activity. *Geochim. Cosmochim. Acta* **73**, 6544–6564.

Vieillard P., Blanc P., Fialips C. I., Gailhanou H. and Gaboreau S. (2011) Hydration thermodynamics of the SWy-1 montmorillonite saturated with alkali and alkaline-earth cations: A predictive model. *Geochim. Cosmochim. Acta* **75**, 5664–5685.

Vieillard P., Gailhanou H., Lassin A., Blanc P., Bloch E., Gaboreau S., Fialips C. I. and Madé B. (2019) A predictive model of thermodynamic entities of hydration for smectites: Application to the formation properties of smectites. *Appl. Geochem.* **110**, 104423.

Vinci D., Dazas B., Ferrage E., Lanson M., Magnin V., Findling N. and Lanson B. (2020) Influence of layer charge on hydration properties of synthetic octahedrally-charged Na-saturated trioctahedral swelling phyllosilicates. *Appl. Clay Sci.* **184**, 105404.

Whittaker M. L., Lammers L. N., Carrero S., Gilbert B. and Banfield J. F. (2019) Ion exchange selectivity in clay is controlled by nanoscale chemical–mechanical coupling. *Proc. Natl. Acad. Sci.* **116**, 22052–22057.

Woodruff W. F. and Revil A. (2011) CEC-normalized clay-water sorption isotherm. *Water Resour. Res.* **47**.

Associate editor: Carl Steefel